

Observation of Motion Dependent Nonlinear Dispersion with Narrow Linewidth Atoms in an Optical Cavity

Philip G. Westergaard^{1,2,*}, Bjarke T. R. Christensen¹, David Tieri³, Rastin Martin¹, John Cooper³, Murray Holland³, Jun Ye³, and Jan W. Thomsen¹

¹*Niels Bohr Institute, University of Copenhagen; Blegdamsvej 17, 2100 Copenhagen, Denmark*

²*Danish Fundamental Metrology; Matematiktorvet 307, 1. sal, 2800 Kgs. Lyngby, Denmark*

³*JILA, National Institute of Standards and Technology and University of Colorado, Boulder, CO 80309-0440, USA*

As an alternative to state-of-the-art laser frequency stabilisation using ultra-stable cavities, it has been proposed to exploit the non-linear effects from coupling of atoms with a narrow atomic transition to an optical cavity. Here we have constructed such a system and observed non-linear phase shifts of a narrow optical line by strong coupling of a sample of strontium-88 atoms to an optical cavity. The sample temperature of a few mK provides a domain where the Doppler energy scale is several orders of magnitude larger than the narrow linewidth of the optical transition. This makes the system sensitive to velocity dependent multi-photon scattering events (Dopplerons) that affect the cavity transmission significantly while leaving the phase signature relatively unaffected. By varying the number of atoms and the intra-cavity power we systematically study this non-linear phase signature which displays roughly the same features as for much lower temperature samples. This demonstration in a relatively simple system opens new possibilities not only for alternative routes to laser stabilization, but also for superradiant laser sources involving narrow line atoms.

PACS numbers: 32.80.Wr, 37.30.+i, 42.50.Ct, 42.62.Fi

State-of-the-art atomic clocks rely on highly coherent light sources to probe narrow optical transitions [1–5]. However, these clocks are limited by the frequency noise of the interrogation oscillator through the Dick effect [6]. Only recently multi-atom optical clocks have surpassed single ion clocks in stability owing to the enhanced laser stability [1, 2, 7]. Achieving a better stability has so far been hampered by thermal noise in the reference cavity used for laser stabilization [8–10]. Recent proposals suggest an alternative approach to laser stabilisation [11–13] where atoms in an optical lattice are probed on the narrow clock transition inside an optical cavity. This brings non-linear effects into the system dynamics that could considerably enhance the spectral sensitivity and potentially lead to laser stability comparable to or better than the current state-of-the-art. However, for finite temperature samples of atoms the principal mechanisms that are relevant to this physical domain have not been investigated in detail.

To achieve a better understanding of cavity-mediated effects with a narrow optical transition we have constructed a system with ^{88}Sr atoms probed on the $|^1\text{S}_0\rangle - |^3\text{P}_1\rangle$ transition at 689 nm inside an optical cavity (see Fig. 1). To capture the basic physics of the strong non-linear phenomena one can consider N atomic dipoles strongly coupled to a single mode of the cavity field. The dipole moment associated with this narrow transition is around five orders of magnitude smaller than that for a typical dipole-allowed transition in an alkaline element. Also, at finite temperature only a small fraction of the atomic sample is probed due to Doppler broadening. Here, the role of the cavity is to enhance the weak interaction by order of the finesse of the cavity.

Experimentally we operate in the so-called "bad cavity" regime, where the atomic dipole decay rate is a factor of 1000 smaller than the cavity decay rate κ . In our experiment we use the ^{88}Sr $|5s^2\ ^1\text{S}_0\rangle - |5s5p\ ^1\text{P}_1\rangle$ transition at 461 nm to cool and trap atoms in a magneto-optical trap (MOT). We load about 5×10^8 atoms in the MOT at a temperature of 2 – 4 mK inside an optical cavity prepared for light at 689 nm. The cavity waist of $w_0 = 500\ \mu\text{m}$ ensures a good overlap with the MOT and negligible transit time broadening (~ 2 kHz) compared to the natural line width ($\Gamma/2\pi = 7.6$ kHz) of the probe transition. The dimensionless number $C = C_0N$, where $C_0 = 4g^2/\Gamma\kappa$ depends on the single-atom/cavity coupling constant g , is known as the collective cooperativity and is a measure of how strong the coherent atom-cavity coupling is with respect to the dissipation channels. In our configuration we are able to generate a collective cooperativity of about $C = 630$, thus placing our system in the strongly coupled regime.

Our experiment is operated in a cyclic fashion. We start each cycle preparing the atomic sample by loading a MOT inside the optical cavity. After loading we shut off the MOT beams and probe the atoms at 689 nm while recording both the intensity and phase shift of the transmitted probe light via two detectors (see Fig. 1). The total cycle time is typically around 0.5 – 1 s. For the phase measurement we employ cavity-enhanced FM spectroscopy by using the so-called noise-immune cavity-enhanced optical-heterodyne molecular spectroscopy (NICE-OHMS) technique [14, 15] (see Supplemental Information). This technique has a clear advantage over heterodyne signals generated, for example, from interferometric methods in terms of superior noise

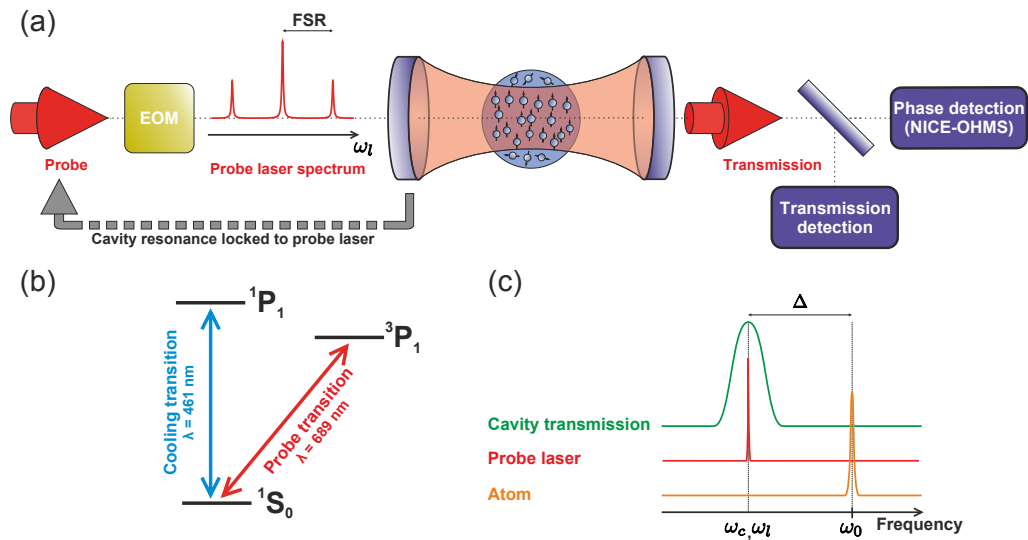


FIG. 1. (color online). (a) Experimental setup. A sample of cold atoms (MOT) is prepared inside a low finesse cavity ($F = 85$) which is held at resonance with the probe laser. We probe the atoms on the inter-combination line $|5s^2\ ^1S_0\rangle - |5s5p\ ^3P_1\rangle$ at 689 nm ($\Gamma/2\pi = 7.6$ kHz). Both intensity and phase shift of the transmitted probe light are recorded. The phase is measured relative to the input field by employing cavity-enhanced heterodyne spectroscopy (NICE-OHMS). (b) Energy levels of the ^{88}Sr atom and transitions relevant for this work. (c) Relation between the spectral components in the experiment. The probe laser frequency ω_l (and consequently the cavity resonance ω_c) is detuned a variable amount Δ with respect to the atomic resonance ω_0 .

reduction and simplicity. During experiments we lock the cavity resonance to the 689 nm laser frequency using a Hänsch-Couillaud scheme [16]. The standing wave generated in the cavity will thus be present at all times while the 689 nm laser frequency is scanned.

In the limit of $T = 0$ and for very low cavity field intensities several solutions exist for the steady-state intra-cavity field [13]. This is known as optical bi-stability, which would render the system unsuited for frequency stabilisation. However, at finite temperatures this picture changes. Above a critical temperature T_{crit} only one solution for the steady-state intra-cavity field exists. For our parameters T_{crit} is of the order of a few hundred nK while experiments are typically performed at mK temperatures.

The non-zero velocity of the atoms brings additional photon resonance phenomena into play that profoundly changes the complex amplitude of the cavity field around the atomic resonance ω_0 . In the rest frame of an atom moving with velocity v_j the atom experiences a bi-chromatic light field given by $\omega_+ = \omega_l(1 + v_j/c)$ and $\omega_- = \omega_l(1 - v_j/c)$, where ω_l is the laser frequency and c is the speed of light. Resonant scattering events will take place if the atom is Doppler-tuned into resonance at ω_0 , e.g., $\omega_- = \omega_0$, such that the atom may absorb a photon from a given direction of the cavity field. Higher order resonances are also possible where, e.g., the atom absorbs two photons from one direction at ω_- and emits one photon in the other direction at ω_+ . Generally, the resonance condition becomes $(p + 1)\omega_- = \omega_0 + p\omega_+$

for $p = 0, 1, 2, \dots$. The process is illustrated in Fig. 2(a). These non-linear multi-photon scattering effects are known as Dopplerons and give rise to a series of velocity dependent resonances [17], which change the transmitted field amplitude around resonance.

In Fig. 2(b, c) we show typical results for a frequency scan across the $|^1S_0\rangle - |^3P_1\rangle$ line resonance (red circles). The input power was 975 nW corresponding to an average saturation parameter of $S_0 = 618$. It is clear that the phase signal in Fig. 2(c) has a significantly higher signal-to-noise ratio ($S/N = 70$) than the transmitted power signal in Fig. 2(b) ($S/N \sim 4$), demonstrating the effectiveness of the NICE-OHMS technique. Currently, the factor limiting the signal-to-noise ratio of the phase signal is the shot-to-shot atom number fluctuations and residual amplitude modulation from the EOM.

We model the dynamics of the system by a Hamiltonian describing the coherent time evolution of an ensemble of atoms, where each atom with a given velocity is coupled to a single mode of the optical cavity. Solving the corresponding optical Bloch equations yields the cavity-transmitted intensity and phase as a function of detuning, number of atoms, and temperature. Our model is also adapted to take into account the spatial extent of the cavity field and atomic density profile. The blue solid curves in Fig. 2 (b, c) are the theoretical prediction based on the Hamiltonian presented in Supplemental Equation 2 (see Supplemental Information for details). In our theoretical model we fix the number of atoms, laser input power, laser line width, cavity waist, and cavity finesse

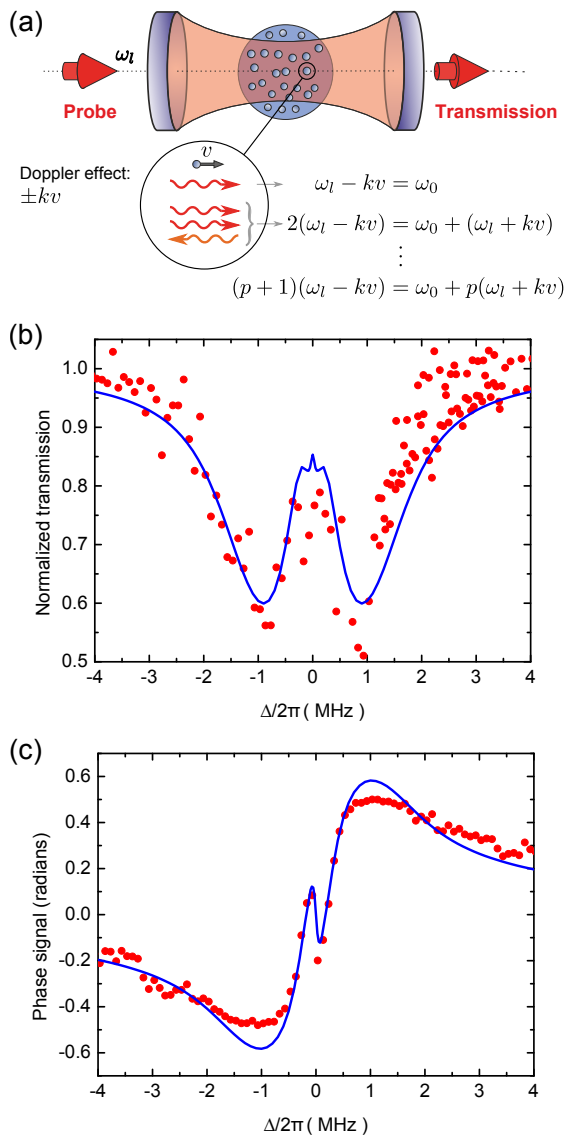


FIG. 2. (color online). (a) Illustration of the Doppleron multi photon processes that take place in our system. We consider a given atom with velocity component v in the direction of the cavity axis. (b, c) Typical frequency scan without any averaging across the atomic resonance for an input power of 975 nW and a total number of atoms in the MOT of $N = 4.4 \cdot 10^8$. The data in (b) displays the transmission of the probe light through the cavity normalized to a signal with no atoms in the cavity. The data in (c) is the phase shift of the cavity-transmitted field obtained using the NICE-OHMS method. The solid lines are theoretical predictions based on our theoretical model which includes the Doppler effect and the spatial overlap of the thermal cloud (here with temperature $T = 2.3$ mK) with the cavity field. At maximum phase shift (around detunings of $\Delta \simeq \pm 1$ MHz) our detection system starts to saturate giving a slightly flatter appearance of the phase data.

based on experimental values, but allow a scaling factor for the absolute phase. The temperature is allowed to vary in the range of 2-4 mK, in accordance with the experimental condition.

Considering the transmission in Fig. 2(b) we can identify three spectral features: (1) the broad (~ 3 MHz wide) Doppler absorption feature consistent with the sample temperature of a few mK; (2) a central region (~ 1 MHz wide) with enhanced transmission due to saturation, but affected by the Doppleron resonances which lead to enhanced back-scattering (or reduced forward transmission), limiting the height of the saturated absorption peak; (3) finally, in the central region around zero velocity (i.e., on resonance), the Doppleron mechanism breaks down and the saturated absorption takes place again with increased transmission as a result.

The effect of the Dopplerons is not so readily apparent in the phase signal (Fig. 2(c)). Here, the most dominant features are the dispersion from the Doppler broadened absorption and the dispersion from the central saturated absorption peak with inverted slope. However, the Dopplerons do have an observable effect on the phase signature which is a rounding of the curvature around the central dispersion feature, consistent with our theoretical model.

It is interesting to compare the situation observed in Fig. 2(b) and Fig. 2(c) against lower temperature results. In Fig. 3 we plot theoretical transmission and phase curves for $T = 4$ mK, $T = 400 \mu\text{K}$ and $T = 40 \mu\text{K}$, where $T = 4$ mK corresponds to the typical experimental situation. The effect of going to lower temperature is evident on the transmission curves, where the Dopplerons become less and less dominant. The phase is less affected by Dopplerons, although the slope on resonance tends to increase slightly with decreasing temperature. The slope around zero-frequency determines the potential stability of this system in application as a frequency-lock. However, considering the additional experimental complexity of decreasing the temperature by orders of magnitude and the possible reduction of atom number in the process, the gain in slope is minimal.

To evaluate and characterize our physical system experimentally we have mapped out the central phase feature as a function of probe input power with fixed atom number. In Fig. 4 we show the phase signal for a fixed number of atoms as a function of laser detuning for different input powers in the range 650 - 1950 nW. For high input powers we strongly saturate the dipole and power broaden the central saturated absorption peak. As we gradually lower the input power, the power broadening is reduced leaving the central phase feature with a larger slope without reducing the signal-to-noise ratio.

Fig. 5 (a) - (d) shows the evolution of the phase signal for fixed probe power as the number of atoms inside the cavity mode is changed from $N_{\text{cavity}} = 2.5 \times 10^7$ in (a) to $N_{\text{cavity}} = 1.2 \times 10^7$ in (d). Despite being strongly satu-

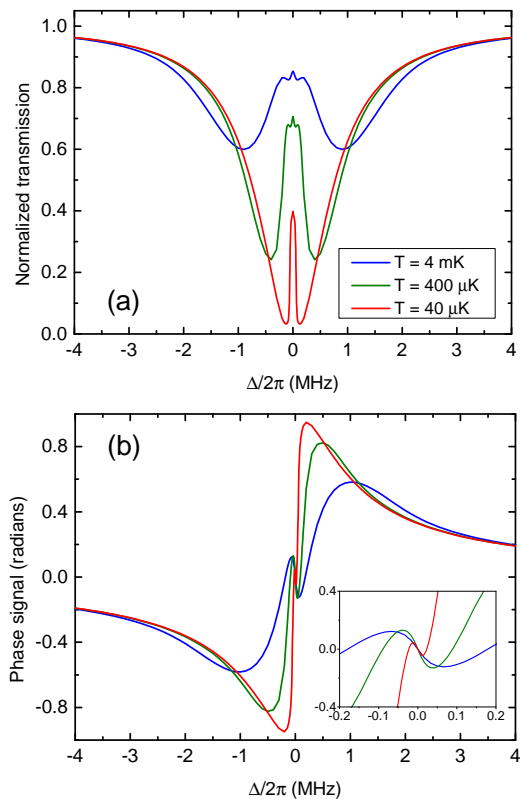


FIG. 3. (color online). Theoretical plots of the variation of the transmission (a) and the phase (b) with the temperature of the atoms. The input power and number of atoms are the same as in Fig. 2. The temperature $T = 4$ mK corresponds to a typical experimental situation. The inset in (b) shows a zoom on the central part of the plot with the same units on the axes.

rated and in a finite temperature regime the atomic phase signature is not significantly influenced (deteriorated) by the Doppler resonances in contrast to the transmission profile. We observe a strong dependence on atom number with increasing phase response and increasing slope on resonance for increasing atom numbers as expected.

In conclusion, we have constructed a system dominated by highly saturated multi-photon absorption with laser-cooled strontium atoms coupled to a low-finesse optical cavity. The transmission through the cavity is strongly altered by thermal effects and Dopplerons, but the central phase response of the atoms remains relatively immune to these effects while displaying a high signal-to-noise ratio (SNR) owing to the cavity and detection technique. The atomic phase signature was observed via cavity enhanced FM spectroscopy (NICE-OHMS) on the narrow optical $|^1S_0\rangle - |^3P_1\rangle$ inter-combination line of ^{88}Sr providing SNR of exceeding 7000 for one second of integration. We observe a strong dependence on atom number and intensity of the cavity field and we are able to change the dispersion shape by tuning these param-

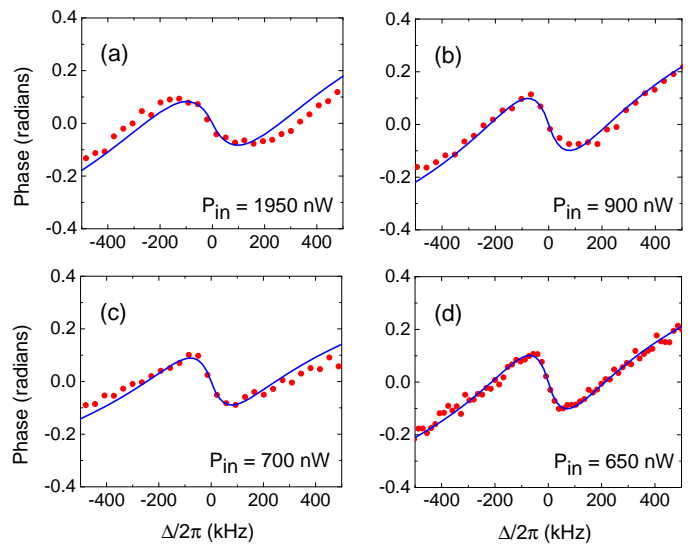


FIG. 4. (color online). Measured phase shift of the cavity-transmitted field when scanned across the atomic resonance. The input probe laser power P_{in} is progressively decreased from 1950 nW (a) to 650 nW (d). The number of atoms is about $N_{\text{cavity}} = 2.5 \times 10^7$. Each point is an average of 3 data points. The solid lines are theoretical predictions based on our theoretical model.

eters, in accordance with our theoretical model that includes finite temperature effects and multi-photon scattering events. The understanding obtained here of the "bad cavity" physics lends promise to further development in this area, such as a new generation of frequency stabilisation [11, 13] or superradiant laser sources [18, 19].

We would like to acknowledge support from the Danish research council and ESA contract number No. 4000108303/13/NL/PA-NPI272-2012. DT, MH, and JY also wish to thank the DARPA QuASAR program, the NIST and the NSF for financial support.

* pgw@dfm.dk

- [1] B. J. Bloom *et al*, *Nature* **506**, 71-75 (2014).
- [2] N. Hinkley *et al*, *Science* **341**, 1215-1218 (2013).
- [3] R. Le Targat *et al*, *Nat. Commun.* **4**, 2109 (2013).
- [4] M. Takamoto, F.-L. Hong, R. Higashi, and H. Katori, *Nature* **435**, 321-324 (2005).
- [5] C. W. Chou, D. B. Hume, J. C. J. Koelemeij, D. J. Wineland, and T. Rosenband, *Phys. Rev. Lett.* **104**, 070802 (2010).
- [6] G. Santarelli, C. Audoin, A. Makdissi, P. Laurent, G. J. Dick, and A. Clairon, *IEEE Trans. Ultrason. Ferroelectr. Freq. Control* **45**, pp. 887-894 (1998).
- [7] T. L. Nicholson, M. J. Martin, J. R. Williams, B. J. Bloom, M. Bishof, M. D. Swallows, S. L. Campbell, and J. Ye, *Phys. Rev. Lett.* **109**, 230801 (2012).
- [8] T. Kessler, T. Legero, and U. Sterr, *J. Opt. Soc. Am. B* **29**, 178-184 (2012).

- [9] T. Kessler *et al*, *Nature Photonics* **6**, 687-692 (2012).
 [10] M. J. Martin *et al*, *Science* **341**, 632-636 (2013).
 [11] D. Meiser, J. Ye, D. R. Carlson, and M. J. Holland, *Phys. Rev. Lett.* **102**, 163601 (2009).
 [12] D. Meiser and M. J. Holland, *Phys. Rev. A* **81**, 033847 (2010).
 [13] M. J. Martin, D. Meiser, J. W. Thomsen, J. Ye, and M. J. Holland, *Phys. Rev. A* **84**, 063813 (2011).
 [14] J. Ye, L.S. Ma, and J. L. Hall, *J. Opt. Soc. Am. B* **15**, 6-15 (1998).
 [15] L. S. Ma, J. Ye, P. Dubé, and J. L. Hall, *J. Opt. Soc. Am. B* **16**, 2255-2268 (1999).
 [16] T. W. Hänsch and B. Couillaud, *Opt. Commun.* **35**, 441-444 (1980).
 [17] E. Kyrölä and S. Stenholm, *Opt. Commun.*, **22**, 123 (1977).
 [18] J. G. Bohnet, Z. Chen, J. M. Weiner, D. Meiser, M. J. Holland, and J. K. Thompson, *Nature*, **484**, 78-81 (2012).
 [19] T. Maier, S. Kraemer, L. Ostermann, and H. Ritsch, *Opt. Express* **22**, 13269 (2014).

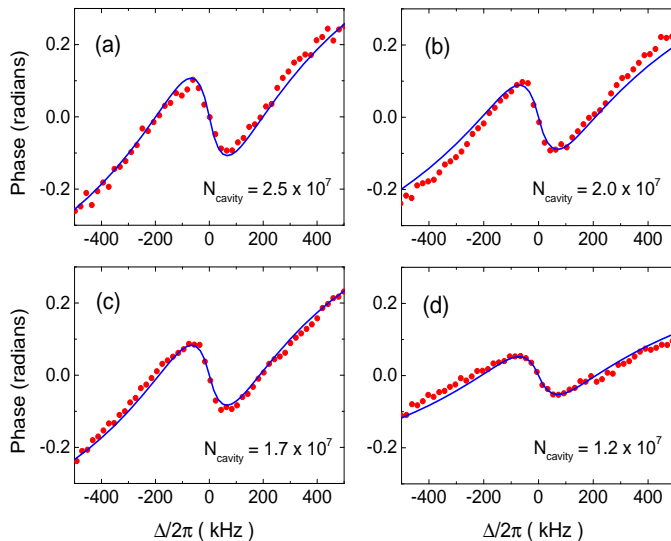


FIG. 5. (color online). Measured phase shift of the probe light when scanned across the atomic resonance. The number of atoms in the cavity is progressively decreased from from 2.5×10^7 (a) to 1.2×10^7 (d). The input power used for all plots was 650 nW. Each point is an average of 3 data points. The solid lines are theoretical predictions based on our theoretical model.

SUPPLEMENTAL INFORMATION

Detection Scheme

After loading the MOT for 0.5 – 1 s we shut off the MOT beams and wait for 100 μ s before probing the atoms for 100 μ s. The probe laser beam is split up after the cavity and sent to two detectors which allow for a low bandwidth detection (50 MHz) of the transmitted power and a high bandwidth detection (2000 MHz) for the phase measurement. The NICE-OHMS phase signal is obtained by generating Fourier sidebands in the probe light at exactly the free spectral range (FSR) of our cavity at 500 MHz using an EOM. The carrier is tuned close to the atomic resonance and will experience a phase shift due to the atoms. The sidebands, on the other hand, are far off resonance and will not be influenced by the atoms. They will, however, still be transmitted through the cavity since they are displaced by exactly one FSR, and experience similar technical noise and low-frequency amplitude noise as the carrier. Demodulating the heterodyne beat signal between the carrier and the sidebands after the high bandwidth detector will result in a signal proportional to the phase shift induced by the atoms at a significantly reduced noise level.

The transmission is measured by normalising the signal from the slow detector obtained just after the MOT is shut off with a signal obtained after waiting an additional 50 ms for all the atoms to have left the cavity. To minimize frequency fluctuations of the 689 nm laser we lock the laser to a high finesse ULE cavity ($F \sim 8000$) using the Pound-Drever-Hall method [1]. At 1 ms of integration time the laser has a linewidth of about 600 Hz.

We monitor the number of atoms through the atomic absorption (low bandwidth detector) and indirectly through the MOT fluorescence measured by a photomultiplier. Typically, we trap about 5×10^8 atoms in the MOT while only $N_{\text{cavity}} = 2 \times 10^7$ atoms overlap with the cavity volume. The number of atoms is tuned by changing the loading time of the MOT.

Experimental Parameters

By optical alignment of the MOT beams the trap center is off-set from the quadrupole magnetic field zero such that atoms experience a constant magnetic field of about 1 mT aligned parallel to the probe light polarization. This provides a local quantization axis and ensures that we only probe the π -transition; the σ^\pm transitions are shifted by tens of MHz. The mirrors for the 689 nm cavity are attached outside the view ports of the vacuum chamber, limiting the finesse of the cavity to $F = 85$ and the cavity length to $L = 30$ cm.

Our atom-cavity parameters are characterized by the atom-light coupling g , probe cavity decay time constant

κ and atomic decay time constant Γ which are given by $(g, \kappa, \Gamma) = 2\pi \times (1.50 \text{ MHz}, 5.8 \text{ MHz}, 7.6 \text{ kHz})$. The coupling constant g refers to atoms that have a near-zero velocity component along the probe field k -vector ($N = 3 - 5 \times 10^6$) and not the entire thermal sample overlapping the mode volume ($N_{\text{cavity}} = 2 \times 10^7$). The cavity linewidth $\kappa/2\pi = 6 \text{ MHz}$ is about a factor of 800 larger than the atomic linewidth $\Gamma/2\pi = 7.6 \text{ kHz}$ leaving the system in the so-called ‘‘bad cavity’’ regime.

Theoretical Model

We model our system as a collection of 2-level atoms inside a single mode optical cavity, using a Born-Markov master equation to describe the open quantum system,

$$\frac{d}{dt}\hat{\rho} = \frac{1}{i\hbar} [\hat{H}, \hat{\rho}] + \hat{\mathcal{L}}[\hat{\rho}], \quad (1)$$

where,

$$\begin{aligned} \hat{H} = & \frac{\hbar\Delta}{2} \sum_{j=1}^N \hat{\sigma}_j^z + \hbar\eta (\hat{a}^\dagger + \hat{a}) \\ & + \hbar \sum_{j=1}^N g_j(t) (\hat{a}^\dagger \hat{\sigma}_j^- + \hat{\sigma}_j^+ \hat{a}). \end{aligned} \quad (2)$$

The Hamiltonian H describes the coherent evolution of the coupled atom cavity system in an interaction picture which rotates at the frequency of the cavity, and $\Delta = \omega_a - \omega_c$ is the atom-cavity detuning. The Pauli spin matrices are $\hat{\sigma}_j^{+, -, z}$, η is the classical drive amplitude $\eta = \sqrt{\frac{\kappa P_{in}}{\hbar\omega}}$, with P_{in} being the input optical power, and \hat{a} is the annihilation operator of the cavity mode. The atom-cavity coupling rate is given by:

$$g_j(t) = g_0 \cos(kz_j - \delta_j t) e^{-r_j^2/w_0^2}, \quad (3)$$

where k is the wave number of the cavity, z_j and r_j are the longitudinal and axial positions, $\delta_j = kv_j$ is the Doppler shift in terms of the atom velocity v_j , w_0 is the waist of the gaussian cavity mode, and $g_0 = \wp/\hbar\sqrt{\hbar\omega_c/2\varepsilon_0 V_{\text{eff}}}$ the vacuum Rabi frequency with V_{eff} the effective mode volume of the cavity, \wp the dipole moment of the atomic transition, and ε_0 the vacuum permittivity.

The incoherent evolution is described by the Liouvillian $\hat{\mathcal{L}}[\hat{\rho}]$,

$$\begin{aligned} \hat{\mathcal{L}}[\hat{\rho}] = & -\frac{\kappa}{2} \{ \hat{a}^\dagger \hat{a} \hat{\rho} + \hat{\rho} \hat{a}^\dagger \hat{a} - 2\hat{a} \hat{\rho} \hat{a}^\dagger \} \\ & -\frac{\gamma}{2} \sum_{j=1}^N \{ \hat{\sigma}_j^+ \hat{\sigma}_j^- \hat{\rho} + \hat{\rho} \hat{\sigma}_j^+ \hat{\sigma}_j^- - 2\hat{\sigma}_j^- \hat{\rho} \hat{\sigma}_j^+ \} \\ & + \frac{1}{2T_2} \sum_{j=1}^N \{ \hat{\sigma}_j^z \hat{\rho} \hat{\sigma}_j^z - \hat{\rho} \}, \end{aligned} \quad (4)$$

where κ is the decay rate of the cavity, γ is the spontaneous emission rate for the atoms, and $1/(2T_2)$ is the inhomogeneous dephasing.

We derive c -number Langevin equations corresponding to equation (1). Assuming that the classical drive η is strong enough a mean-field description provides an accurate representation. We therefore define the mean values $\alpha = i \langle \hat{a} \rangle$, $\sigma_j^- = \langle \hat{\sigma}_j^- \rangle$, $\sigma_j^+ = \langle \hat{\sigma}_j^+ \rangle$, $\sigma_j^z = \langle \hat{\sigma}_j^z \rangle$ which evolve according to

$$\dot{\alpha} = -\kappa\alpha + \eta + \sum_{j=1}^N g_j(t) \sigma_j^-, \quad (5)$$

$$\dot{\sigma}_j^- = -\left(\frac{1}{T_2} + i\Delta\right) \sigma_j^- + g_j(t) \alpha \sigma_j^z, \quad (6)$$

$$\dot{\sigma}_j^z = -\gamma(\sigma_j^z + 1) - 2g_j(t) (\alpha \sigma_j^+ + \alpha^* \sigma_j^-). \quad (7)$$

In the moving frame of reference of each atom, the cavity field appears as a travelling wave, containing two frequencies shifted above and below the cavity frequency by the Doppler shift. To solve this problem that intrinsically contains a bi-chromatic drive we proceed in two ways.

We first numerically integrate equations (5) - (7), approximating the sum in equation (5) as an integral, with the integrand weighted by the thermal velocity distribution. The integral is then partitioned into finite segments. The positions are chosen in an analogous manner, with the atoms being distributed in a gaussian distribution of width $2w_0$ by the MOT. The velocity partition must be chosen with care, since the system exhibits doppleron resonances. Specifically, at lower velocity, more resolution in the partition is required.

We also do a floquet analysis [2], in which we define for each atom,

$$\begin{aligned} \sigma^- &= \sum_l e^{il\delta t} x_1^{(l)}, \\ \sigma^+ &= \sum_l e^{il\delta t} x_2^{(l)}, \\ \sigma^z &= \sum_l e^{il\delta t} x_3^{(l)}, \end{aligned}$$

Upon substitution into equations (5-7), equations for the amplitudes $x_1^{(l)}$, $x_2^{(l)}$, and $x_3^{(l)}$ are found:

$$\dot{x}_1^{(l)} = -\left(i(\Delta + l\delta) + \frac{1}{T_2}\right) x_1^{(l)} + \frac{\alpha}{2} \left(\beta x_3^{(l+1)} + \beta^* x_3^{(l-1)}\right), \quad (8)$$

$$\dot{x}_2^{(l)} = \left(i(\Delta + l\delta) - \frac{1}{T_2}\right) x_2^{(l)} + \frac{\alpha^*}{2} \left(\beta^* x_3^{(l+1)} + \beta x_3^{(l-1)}\right), \quad (9)$$

$$\begin{aligned} \dot{x}_3^{(l)} &= -\gamma \delta_{l,0} - (il\delta + \gamma) x_2^{(l)} \\ &\quad - \left(\beta \alpha x_2^{(l+1)} + \beta \alpha^* x_1^{(l+1)} + \beta^* \alpha x_2^{(l-1)} + \beta^* \alpha^* x_1^{(l-1)}\right), \end{aligned} \quad (10)$$

where

$$\beta = g_0 e^{ikz} e^{-\frac{x^2}{w_0^2}}. \quad (11)$$

For a given α , Equations (8 - 10) define a linear system of equations, which are solved by truncating l at some finite value, and inverting the system.

In the steady state, equation (5) becomes,

$$0 = -\kappa\alpha + \eta + \frac{g_0 N}{2} \int_{-\infty}^{\infty} d\delta P(\delta) \left(\beta x_1^{(-1)} + \beta^* x_1^{(1)}\right), \quad (12)$$

where the sum over atoms has again been approximated as in integral, and $P(\delta)$ is the thermal velocity distribution. The α that solves equation (12) is found by applying Newton's method for root finding. We see excellent agreement between the two methods.

* pgw@dfm.dk

- [1] R. W. P. Drever *et al*, *Appl. Phys. B* **31**, Issue 2, 97-105 (1983).
 [2] Z. Ficek and H.S. Freedhoff, *Phys. Rev. A* **48**, 3092-3104 (1993).